

Self-conjugation of the edge diffraction wave using a quadric hologram

GALINA V. BOGATRYOVA, PETER V. POLYANSKII

Department of Correlation Optics, Chernivtsy University, ul. Kotsyubinsky 2, 274012 Chernivtsy, Ukraine.

Self-conjugation of the wave front corresponding to a near-field diffraction of a simple primary wave by an aperture has been realized. Such an operation is performed by using a static hologram that is nonlinearly recorded with a standing reference wave. The contouring effect at the self-conjugated reconstruction is demonstrated. This effect is interpreted within the framework of the Young–Rubinowicz concept of diffraction phenomena, namely, as the result of predominant phase conjugation of the edge diffraction wave.

1. Introduction

Various techniques of the phase conjugation (PC) are employed in optics. The PCs based on a simulated Brillouin back-scattering (SBS-PC) and on the four-wave degenerate mixing process (FWM-PC) by means of the dynamic holography – photorefractive nonlinear optics – dominate among them [1], [2]. Recently, an optical PC of the object's wave front has been implemented by POLYANSKII [3] by means of static holography, using a quadric hologram (QH) technique.

The term “quadric hologram” has been coined for a hologram whose peculiar reconstruction properties are caused just by the quadratic component of the power series expansion of a hologram's complex amplitude response $T_a(\vec{r})$, with respect to the exposure (or intensity) degrees [4]

$$T_a(\vec{r}) = \sum_{l=0}^2 T_l I^l(\vec{r}) \quad (1)$$

where: $T_l = c_l t^l$, $c_l = \frac{1}{l!} \frac{\partial^l T_a}{\partial E^l}$, $E(\vec{r}) = tI(\vec{r})$; t is an exposure time, $I(\vec{r})$ is the intensity of an exposing field, and \vec{r} is the position vector of the running point at the registration domain.

The recording arrangement of the QH-based PC-mirror (QH-PCM) is the same as the well-known arrangement of the FWM using two counterpropagating pumping beams. However, unlike the dynamic holography approach where a photorefractive hologram is read out “in opposed ray tracing-manner” by each of the pumping beams, the QH-PCM operates in the *self-conjugated* fashion, just as the SBS-PC: the object wave is partially re-scattered in its own phase-conjugated replica,

without participation of any of the two reference waves in the readout process. It is important, on the other hand, that the formation of a seed of the spontaneous light-scattering in the material exhibiting the SBS-PC is fundamentally preconditioned by the spatial inhomogeneity of the exposing beam, that regularly presumes a diffuser to be placed at the input plane, and a "coded" (speckled) wave front obeying the Gaussian statistics [5], [6] to be self-conjugated. In contrast, the QH-PCM makes it possible to self-conjugate the wave fronts of arbitrary complexity: both the speckled object fields and simple ones, kind of planar or spherical waves. This property of a QH is determined by the use of two reference waves at the recording stage. Namely, the cross-gratings produced by interference of an object wave with each component of a standing reference wave undergo nonlinear mixing (spatial-frequency heterodyning [3], [4]) due to nonlinear amplitude response of a hologram to exposure. The resulting set of the combination gratings in the volume of such a hologram just realizes spatial inhomogeneity of a hologram's reflectivity of specific kind that provides a self-conjugation of an arbitrary wave front irrespective of its complexity.

In this paper, we study the peculiarities of the QH-based PC for the intermediate case, when the object wave results from a knife-edge diffraction or a near-field aperture diffraction. It is obvious that the object field does not obey Gaussian statistics in this case, being at the same time more complex with respect to the plane or spherical wave. We discuss this problem using physically appealing Young–Rubinowicz concept of diffraction phenomena [7]–[9], *i.e.*, understanding a near-field pattern as a sum of the geometrical optics wave defined within the directly illuminated area only, and the edge diffraction wave (EDW) propagating both into the directly illuminated area and to the geometrical shadow region. Previous consequences of the Young–Rubinowicz concept in holography as well as the technique of Young holograms (*i.e.*, holograms of the EDW) have recently been developed in [10]–[16].

In Section 2, we briefly formulate the QH-based PC principle. The possibility of the EDW being self-conjugated by applying the QH-PCM technique is substantiated in Sec. 3. The experimental demonstration of the QH-based self-conjugation of the EDW is given in Sec. 4. The main results of our study are discussed in Sec. 5 and compared with earlier versions of the Young hologram technique.

2. Principle of the quadric hologram-based phase conjugation

Here we formulate concisely the principle of the QH-based PC following the recent papers [3], [4]. Let us define the object wave at the running point of the recording domain with the position vector \vec{r} as the superposition of N wavelets associated with the optical retransmitters whose ensemble represents the object

$$G(\vec{r}) = \sum_{g=1}^N a_g(\vec{r}) \exp [i(\omega t - \vec{k}_g \vec{r} + \varphi_g)] \quad (2)$$

where a_g , \vec{k}_g , φ_g are the amplitude, the wave vector, and the initial phase of the g -th retransmitter, respectively. Let a QH of the wave (2) be recorded using two counterpropagating reference waves, $\Omega_A(\vec{r})$ and $\Omega_B(\vec{r})$, so that

$$\Omega_A(\vec{r}) + \Omega_B(\vec{r}) = A \exp [i(\omega t - \vec{k}_A \vec{r} + \varphi_A)] + B \exp [i(\omega t - \vec{k}_B \vec{r} + \varphi_B)] \quad (3)$$

where A and B are the (constant) amplitudes, and φ_A , φ_B are the initial phases of partial reference waves, since $\vec{k}_A + \vec{k}_B \equiv 0$ at each point of the recording domain. Intensity of the exposure field takes the form

$$I(\vec{r}) = |\Omega_A(\vec{r}) + \Omega_B(\vec{r}) + G(\vec{r})|^2. \quad (4)$$

Substituting (4) into (1), one finds among numerous summands of the quadratic components of the hologram amplitude response $T_2 I^2(\vec{r})$, the term causing the reconstruction of the PC-replica of the object field in the case where a QH is read out by the object wave [3]

$$\{2T_2(G^*(\vec{r}))^2 \Omega_A(\vec{r}) \Omega_B(\vec{r})\} G(\vec{r}) = a G^*(\vec{r}) \quad (5)$$

where $a = 2T_2 \langle |G(\vec{r})|^2 \rangle AB \exp(\varphi_A + \varphi_B)$ is the complex reflectivity of the PCM, $\langle |G(\vec{r})|^2 \rangle = \sum_{\theta=1}^N a_\theta^2(\vec{r})$ is the object wave's intensity averaged over the ensemble of N retransmitters representing the object [17]. (In the case of a speckled object field, it coincides with the intensity averaged over the registration domain [5]).

Let us note that any real nonlinearly recorded hologram exhibits both the quadratic nonlinearity and the higher-order ones. Therefore, nonlinearities of the orders higher than the quadratic one provide only noise contributions into the PC response of a hologram [4]. However, if the cubic and the higher-order nonlinearities are not too large (that implies the limitations on a QH-PCM's reflectivity and its diffraction efficiency [4]), their effect on the PC response may be neglected. Since the fitting of $T_a(\vec{r})$ in terms of cubic polynomial in $E(\vec{r})$ for a nonlinearly recorded hologram is quite good for most of the holographic photolayers [18] and moreover the cubic component occurs, in practice, to be less than the quadratic one by one or two orders of magnitude [18], the QH-approximation accepted by us is adequate for most of the experimental situations.

A QH-PCM can be recorded both at relatively thin photosensitive layers, such as the standard holographic photoemulsions, and using any volume recording medium exhibiting high angular selectivity. From the wave-vector diagrams shown in Fig. 1, there can be seen those demonstrating the combination grating formation.

An interference of the wavelets associated with two arbitrary object retransmitters whose wave vectors are \vec{k}_θ and \vec{k}_q with the reference waves $\Omega_A(\vec{r})$ and $\Omega_B(\vec{r})$ (with the wave vectors \vec{k}_A and \vec{k}_B , respectively) results in the cross-gratings, $\{G^*(\vec{r}) \Omega_A(\vec{r}) + c.c.\}$ and $\{G^*(\vec{r}) \Omega_B(\vec{r}) + c.c.\}$ (*c.c.* designates the complex conjugation), whose wave vectors are: $\vec{K}_{GA} = \vec{k}_\theta - \vec{k}_A$; $\vec{K}_{QA} = \vec{k}_q - \vec{k}_A$; $\vec{K}_{GB} = \vec{k}_\theta - \vec{k}_B$; $\vec{K}_{QB} = \vec{k}_q - \vec{k}_B$, see Fig. 1a. Figures 1b,c show the wave vectors of the quadratic and combination (summation) gratings resulting from a nonlinear mixing of the transmitting and reflecting partial cross-gratings formed with the corresponding retransmitters:

$$\vec{F}_G^{(+)} = \vec{K}_{GA} + \vec{K}_{GB} \equiv 2\vec{k}_\theta,$$

$$\vec{F}_Q^{(+)} = \vec{K}_{QA} + \vec{K}_{QB} \equiv 2\vec{k}_q,$$

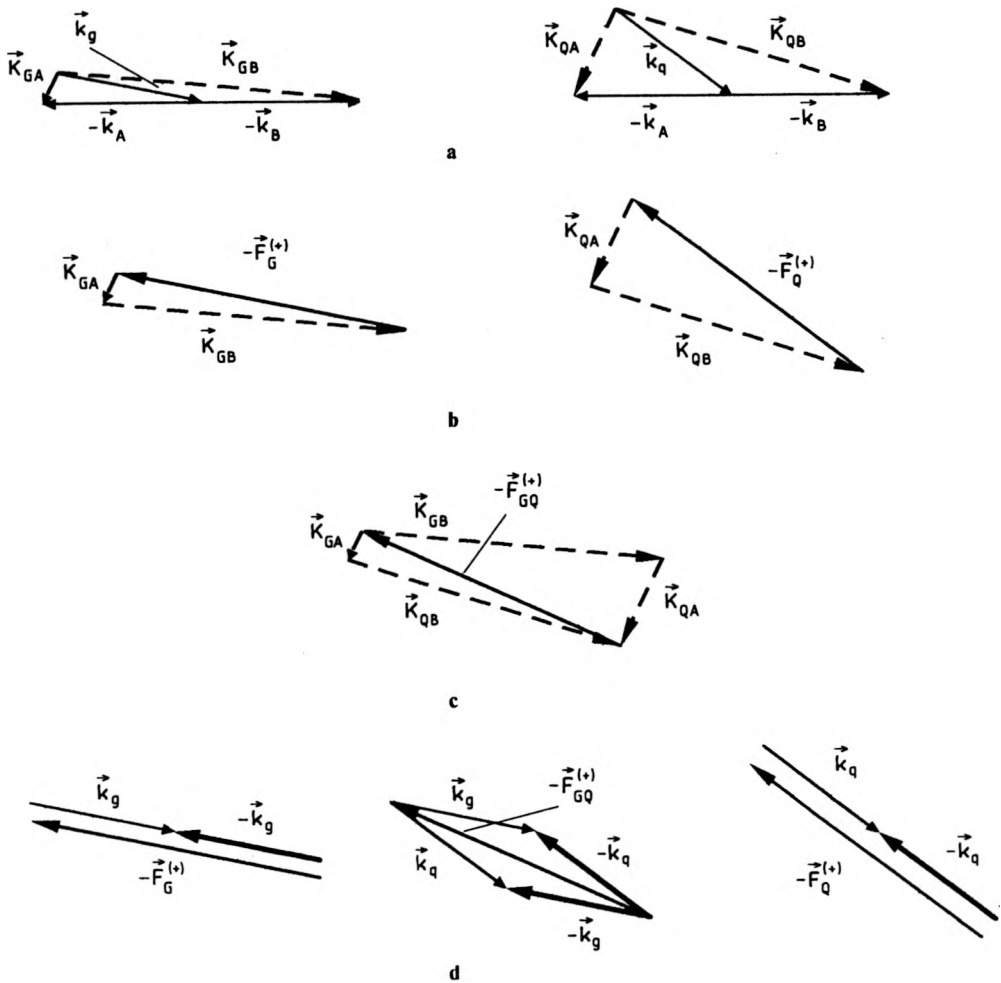


Fig. 1. Wave-vector diagrams explaining the principle of the wave front self-conjugation by using the quadric hologram recorded with two counterpropagating reference waves: \vec{k}_g, \vec{k}_q – the wave vectors associated with wavelets corresponding to arbitrary retransmitters of the object; $-\vec{k}_A = \vec{k}_B$ – the wave vectors of the reference waves ($|\vec{k}_A| = |\vec{k}_B| = |\vec{k}_g| = |\vec{k}_q| = 2\pi/\lambda$); $\vec{K}_{GA}, \vec{K}_{QA}, \vec{K}_{GB}, \vec{K}_{QB}$ – the wave vectors associated with the cross-gratings resulting from interference of the object wave with the reference ones; $\vec{F}_G^{(+)}, \vec{F}_Q^{(+)}, \vec{F}_{GQ}^{(+)}$ – the wave vectors of the summation gratings providing the wave front phase conjugation process.

$$\vec{F}_{GQ}^{(+)} = \vec{K}_{GA} + \vec{K}_{QB} = \vec{K}_{GB} + \vec{K}_{QA} \equiv \vec{k}_g + \vec{k}_q.$$

As is well known [2], [19], [20], the presence of the so-called “ $2k$ ”-gratings is the universal and unambiguous formal sign of the PCM functioning in the self-conjugated fashion. Really, as can be seen from Fig. 1d, the gratings with the wave vectors $\vec{F}_G^{(+)}, \vec{F}_Q^{(+)}$ and $\vec{F}_{GQ}^{(+)}$ satisfy the Bragg condition for the case when a QH is read out by the object wave

$$\vec{k}_q - \vec{F}_Q^{(+)} = -\vec{k}_q; \quad \vec{k}_q - \vec{F}_{GQ}^{(+)} = -\vec{k}_q; \quad \vec{k}_g - \vec{F}_{GQ}^{(+)} = -\vec{k}_g; \quad \vec{k}_g - \vec{F}_G^{(+)} = -\vec{k}_g. \quad (6)$$

It follows from Eqs. (6) and Fig. 1d that diffraction of the wavelet from each object retransmitter in the set of quadratic and summation gratings results in reconstruction of both its own PC-replica and in a PC-replica of another wavelet involved. It grounds the possibility of reconstructing the complete self-conjugated replica of the object by reflection of both the whole object wave $G(\vec{r})$ and its partial version from the QH-PMC, if only the gratings with both the wave vectors $\vec{F}_G^{(+)}$, $\vec{F}_Q^{(+)}$ and the wave vectors $\vec{F}_{GQ}^{(+)}$ are represented in the spatial-frequency structure of a hologram. An associative error-correcting imaging by reflection of the wave produced by incomplete version of the stored memory from a QH-PCM has been demonstrated in [3].

3. Quadric hologram of an edge diffraction wave

3.1. Conceptual background

In this section, we consider the peculiarities of a QH-PC for the case when the object wave $G(\vec{r})$ results from a near-field diffraction of a simple primary wave on a diffraction aperture of arbitrary configuration. In the present discussion, we avoid the rigorous analysis of a wave motion behind a diffraction device. The firm consideration relating to the topic and accounting for the stationary phase principle (SPP) may be found in [21]–[23]. Instead, we will try to explicate some intuitive arguments that may be relevant to a holographic experiment.

In accordance with the Young's heuristic approach [24], [25], the field originating from a diffraction of the primary illuminating wave at any simple aperture (without a diffuser) may be understood as the one resulting from interference of the part of the primary wave whose propagation obeys the geometrical optics laws, and the EDW arising due to the amplitude gradient of the field behind the sharp edge of an opaque obstacle. The comprehensive mathematical background of intuitive Young's notion concerning the nature of diffraction, within the framework of validity of the Kirchhoff's scalar theory, has been given by RUBINOWICZ [7], [8], [26], (see also [9], [21], [24], [25]). Following the Young–Rubinowicz approach, the diffraction field behind the diffraction obstacle is described as the sum

$$G(\vec{r}) = G_g(\vec{r}) + G_d(\vec{r}) \quad (7)$$

where $G_g(\vec{r})$ is the geometrical optics wave at the running point of the observation domain, and $G_d(\vec{r})$ is the EDW generally defined by the integral over the rim of a diffraction obstacle. In accordance with such a representation, the EDW's wave front behind the obstacle is disrupted at the boundary of the directly illuminated area and the geometrical shadow region, and this disrupt exactly compensates for the disrupt of the wave front of the geometrical optics wave, so that the resulting wave motion arises to be continuous. Besides, the EDW is in-phase with the geometrical optics wave within the geometrical shadow region, being out-of-phase by π with this wave at the directly illuminated area [8]. It is well known [8], [12], if the imaging is performed by applying the schlieren technique, such a phase structure of the EDW results in a dark-field image of the diffraction obstacle's rim that is bounded by two

bright fringes being out-of-phase by π . Let us emphasize in this connection that based on the shown double-contouring effect we give preference to the Rubinowicz's approach to explanation of diffraction phenomena against the Keller's approach [27] within which the edge diffraction rays (rather than waves) are postulated but are not derived from the *primary principles*. As it follows from the Rubinowicz's representation of the Kirchhoff diffraction integral, the EDW's amplitude approaches half of an amplitude of the wave impinging on the diffraction device as the observation point runs to the geometrical shadow boundary [8], and rapidly decreases in magnitude (as $[\tan(\vartheta_{\text{diffr}}/2)]^{-1}$, where ϑ_{diffr} is the diffraction angle) as the running point leaves this boundary [9], [21].

One more feature of the model relevant to the following consideration of the holographic problem is derived on the basis of the SPP. Namely, if the well-known prerequisites of the SPP [28], such as "slow" (in a spatial sense) changes of a wave amplitude within the integration domain, and deterministic but fast (owing to a small wavelength) changes of the space-dependent part of a phase factor, quadratic as a rule, are valid, then successive reduction in dimensionality of the representation of the diffraction field takes place [21], resulting in degeneration of the linear integral over the boundary of the diffraction device into contributions of the set (often limited) of the wavelets associated with the critical points of the second kind, localized at the obstacle rim and obeying the peculiar "reflection rule" [7], [9], [25]. Hereinafter, the critical points of the second kind (whose nearest vicinities with linear dimension of the order of the diameter of the central Fresnel zone constructed at the plane of a diffraction device from the recording plane are called the "active zones" [29]) will be referred to as the "edge retransmitters" [10], [16].

3.2. Phase conjugation of the edge diffraction wave

Now we apply the Young–Rubinowicz concept of the EDW to the problem of a self-conjugation of the wave front corresponding to a near-field diffraction using a QH recorded with a standing reference wave.

3.2.1. Edge enhancement at the self-conjugated image

Let us assume that the well-known preconditions of a nonlinear holographic recording [4], [16], [18], such as commensurability of the intensities of the partial reference waves with the object wave intensity, long-time exposure, and over-developing of a photolayer, provide considerable magnitude of the quadratic component of the hologram's amplitude response. In the case under consideration, the following reference-to-object intensity ratio is chosen:

$$|\Omega_A|^2 \approx |\Omega_B|^2 \sim |G_d(\vec{r})|^2 \ll |G_\theta|^2 \quad (8)$$

anywhere within the directly illuminated area (excluding nearest vicinity of the geometrical shadow boundary),

$$|\Omega_A|^2 \approx |\Omega_B|^2 \sim |G_d(\vec{r})|^2 \quad (9)$$

anywhere within the geometrical shadow region (excluding nearest vicinity of the geometrical shadow boundary).

Hereinafter, we omit spatial dependence of intensities of the reference and geometrical optics waves assuming these intensities being constant over the areas where the corresponding waves are defined. At the same time, we hold dependence on \vec{r} for the *complex* (amplitude and phase) distributions as well as relevant spatial dependences in all equations for an EDW.

Substituting Equation (4) with $G(\vec{r})$ specified by Eq. (7) in a power series expansion of the hologram's amplitude response to the exposure degrees (1), one can find, among the terms of this expansion, the components responsible for the self-conjugation of the object wave front:

$$\{2T_2(G_d^*(\vec{r}) + G_g^*(\vec{r}))^2 \Omega_A(\vec{r}) \Omega_B(\vec{r})\} \quad (10)$$

within the directly illuminated area,

$$\{2T_2(G_d^*(\vec{r}))^2 \Omega_A(\vec{r}) \Omega_B(\vec{r})\} \quad (11)$$

within the geometrical shadow region.

Being read out by the part of the object wave propagating into directly illuminated area, $G_d(\vec{r}) + G_g(\vec{r})$, the combination gratings associated with the QH's partial operator (9) give rise to the reconstruction of the component of the self-conjugated response

$$\{2T_2(G_d^*(\vec{r}) + G_g^*(\vec{r}))^2 \Omega_A(\vec{r}) \Omega_B(\vec{r})\} (G_d(\vec{r}) + G_g(\vec{r})) = (\alpha_0 + \alpha_1)(G_d^*(\vec{r}) + G_g^*(\vec{r})) \quad (12)$$

where α_0, α_1 are defined similarly to α in Eq. (5), with $\langle |G(\vec{r})|^2 \rangle$ being replaced by $\langle |G_d(\vec{r})|^2 + |G_g(\vec{r})|^2 \rangle$ and $\{G_d^*(\vec{r})G_g(\vec{r}) + c.c.\}$, respectively. Note that averaging is now performed over the set (if any) of the critical points of the first kind (within the aperture) [21], [29], and the edge retransmitters contributing to the running point of the registration domain with the position vector \vec{r} . The term on the right-hand side of Eq. (12) with α_0 describes the precise PC-reconstruction, while the term with α_1 describes a component of the reconstruction caused by cross-interference of the geometrical optics wave and the EDW which can, in principle, produce an intermodulation noise in the reconstructed image.

Similarly, being read out by the part of the EDW propagating into geometrical shadow region, the combination gratings associated with the QH's partial operator (10) give rise to the reconstruction of the component of the self-conjugated response

$$\{2T_2(G_d^*(\vec{r}))^2 \Omega_A(\vec{r}) \Omega_B(\vec{r})\} G_d(\vec{r}) = \alpha G_d^*(\vec{r}) \quad (13)$$

where α is defined as in Eq. (5), with $\langle |G(\vec{r})|^2 \rangle$ being replaced by $\langle |G_d(\vec{r})|^2 \rangle$.

Let us now compare the diffraction efficiencies of partial QH-PCMs recorded within the directly illuminated area and in the geometrical shadow region. Within the geometrical shadow region, the cross-gratings $\{G_d^*(\vec{r})\Omega_A(\vec{r}) + c.c.\}$ and $\{G_d^*(\vec{r})\Omega_B(\vec{r}) + c.c.\}$ are characterized by the modulation percentages the proportional to the contrasts of partial interference patterns from the EDW and each of the two components of the standing reference wave

$$V_{dA}^{(\text{GSR})}(\vec{r}) = \frac{2|G_d(\vec{r})||\Omega_A|}{(|G_d(\vec{r})|^2 + |\Omega_A|^2 + |\Omega_B|^2)} \quad (14)$$

and

$$V_{dB}^{(\text{GSR})}(\vec{r}) = \frac{2|G_d(\vec{r})||\Omega_B|}{(|G_d(\vec{r})|^2 + |\Omega_A|^2 + |\Omega_B|^2)} \quad (15)$$

respectively. Diffraction efficiency of these *linear* (interferentially produced) cross-gratings will be in proportion to the squared contrast of the corresponding interference pattern, in accordance with the linear holographic theory [18]. At the same time, the modulation percentage of the combination gratings (one of the kind defined by Eq. (10) complemented by its complex conjugation) is always in proportion to the product of the modulation percentages of the constituting cross-gratings [31]. Thus, a partial QH-PCM for the EDW within the geometrical shadow region possesses the diffraction efficiency

$$\eta_d^{(\text{GSR})}(\vec{r}) \sim [V_{dA}^{(\text{GSR})}(\vec{r}) V_{dB}^{(\text{GSR})}(\vec{r})]^2. \quad (16)$$

On the other hand, the cross-gratings $\{G_g^*(\vec{r})\Omega_A(\vec{r}) + c.c.\}$ and $\{G_g^*(\vec{r})\Omega_B(\vec{r}) + c.c.\}$ produced within the directly illuminated area by interference of the geometrical optics wave and each of the two components of the standing reference wave possess the contrasts:

$$V_{gA}(\vec{r}) = \frac{2|G_g||\Omega_A|}{(|G_g|^2 + |G_d(\vec{r})|^2 + |\Omega_A|^2 + |\Omega_B|^2)}, \quad (17)$$

$$V_{gB}(\vec{r}) = \frac{2|G_g(\vec{r})||\Omega_B|}{(|G_g|^2 + |G_d(\vec{r})|^2 + |\Omega_A|^2 + |\Omega_B|^2)}, \quad (18)$$

respectively, while the cross-gratings $\{G_d^*(\vec{r})\Omega_A(\vec{r}) + c.c.\}$ and $\{G_d^*(\vec{r})\Omega_B(\vec{r}) + c.c.\}$ produced within the directly illuminated area by interference of the EDW and each of the two components of the standing reference wave possess the contrasts

$$V_{dA}^{(\text{DIA})}(\vec{r}) = \frac{2|G_d(\vec{r})||\Omega_A|}{(|G_g|^2 + |G_d(\vec{r})|^2 + |\Omega_A|^2 + |\Omega_B|^2)} \quad (19)$$

and

$$V_{dB}^{(\text{DIA})}(\vec{r}) = \frac{2|G_d(\vec{r})||\Omega_B|}{(|G_g|^2 + |G_d(\vec{r})|^2 + |\Omega_A|^2 + |\Omega_B|^2)}, \quad (20)$$

respectively. Thus, a partial QH-PCM for the geometrical optics wave within the directly illuminated area possesses the diffraction efficiency

$$\eta_g(\vec{r}) \sim [V_{gA}(\vec{r}) V_{gB}(\vec{r})]^2 \quad (21)$$

(accounting for Eq. (8), $\eta_g(\vec{r}) \approx \text{const}$, and further we omit spatial dependence of η_g), and a partial QH-PCM for the EDW within this area possesses the diffraction efficiency

$$\eta_d^{(\text{DIA})}(\vec{r}) \sim [V_{dA}^{(\text{DIA})}(\vec{r}) V_{dB}^{(\text{DIA})}(\vec{r})]^2. \quad (22)$$

Finally, the diffraction efficiency of the noise gratings $\{G_d^*(\vec{r}) G_\theta(\vec{r}) + c.c.\}$, (see Eq. (12)) is

$$\eta_{gd}(\vec{r}) \sim [V_{gA}(\vec{r}) V_{dB}^{(\text{DIA})}(\vec{r})]^2 \approx [V_{gB}(\vec{r}) V_{dA}^{(\text{DIA})}(\vec{r})]^2. \quad (23)$$

Accounting for Eqs. (8) and (9), one can estimate the ratios of the diffraction efficiencies of the combination gratings constituting a QH-based PCM

$$\left(\frac{\eta_d^{(\text{GSR})}(\vec{r})}{\eta_\theta} \right) \sim \left[\frac{|G_\theta|}{|G_d(\vec{r})|} \right]^4, \quad (24)$$

$$\left(\frac{\eta_d^{(\text{GSR})}(\vec{r})}{\eta_d^{(\text{DIA})}(\vec{r})} \right) \sim \left[\frac{|G_\theta|}{|G_d(\vec{r})|} \right]^8, \quad (25)$$

$$\left(\frac{\eta_d^{(\text{GSR})}(\vec{r})}{\eta_{gd}(\vec{r})} \right) \sim \left[\frac{|G_\theta|}{|G_d(\vec{r})|} \right]^6. \quad (26)$$

Equations (24)–(26) constitute the definition of a *virtual dark field* [16], [30] incoherent in the PC-reconstructions of QHs from diffraction apertures. Namely, these equations show that the predominant self-conjugation of the part of the EDW propagating into geometrical shadow region is provided by a proper choice of the reference-to-object intensity ratio only, rather than by the use of any “hard” (material) blocking screen. In other words, the dark-field imaging resulting in the edge-enhancement effect at the PC-reconstruction of a QH is realized in the case under consideration by only balancing of the diffraction efficiencies of various combination gratings associated with the quadratic components of the hologram’s amplitude response. It is clear from Eqs. (24)–(26), that $\eta_d^{(\text{DIA})}(\vec{r})$ and $\eta_{gd}(\vec{r})$ may be neglected due to the stronger dependences of the reference-to-object intensity ratios with respect to one for $\eta_d^{(\text{GSR})}$. Let us emphasize that owing to large ratio $\eta_d^{(\text{GSR})}(\vec{r})/\eta_{gd}(\vec{r})$ an intermodulation noise at the PC-response caused by cross-interference of the geometrical optics wave and the EDW (see the text following Eq. (12)) vanishes.

Note that the virtual dark-field effect discussed above is, in consequence, equivalent to the “soft blocking” of DC (direct current) term in Fourier optical systems realized using electron-trapping films [32]. In fact, in both cases, part of the readout radiation propagating to the directly illuminated area (in the case of Fourier-transform hologram, one focused within the central diffraction maximum and its nearest vicinity) is lost, but the apodized pupil function [16] corresponds to the transfer function of the imaging device that provides elimination of undesirable secondary maxima at the resulting contoured image. Obviously, “natural” soft filtering of the DC term by balancing the diffraction efficiencies of partial holographic gratings is preferable, since it does not require the use of any special materials and procedure, being implemented with commercially available high-efficient phase holographic photoplates.

Consider the peculiarities of a near-field QH-based virtual dark-field effect in more detail. In comparison with the well-known classical enhancement of high-frequency

interval of a spatial frequency spectrum by a proper choice of the reference-to-object intensity ratio that is commonly used for optimization of coherent recognition [33]–[35], a QH-based virtual dark-field effect turns out to be much more pronounced. In fact, within the framework of a linear holographic theory [32]–[34], the edge-enhancement effect in a holographic reconstruction is determined by the factor $R \sim [|G_g(\vec{r})| / |G_d(\vec{r})|]^2$, if expressed in terms of the present paper. It means that a linear hologram recorded with the reference-to-object intensity ratio (8) for the exposing waves, being read out by the uniform in intensity *reference* wave, provides R – fold gain of intensity at the image of a rim in comparison with the image of a diffraction aperture. However, if such a hologram is read out by the *object* wave in the matched filtering regime, *i.e.*, if part of a hologram corresponding to the directly illuminated area (with lower diffraction efficiency) is read out by the wave of higher intensity, and part of a hologram corresponding to the geometrical shadow region (with higher diffraction efficiency) is read out by the wave of the lower intensity, then

$$R \left[\frac{|G_d(\vec{r})|^2}{|G_g|^2} \right] \approx 1, \quad (27)$$

so that the resulting intensity of the image of the edge is only “pulled” to the intensity of the image of the aperture. In other words, the edge is enhanced at the image but is not dominating in intensity. On the contrary, a QH-based self-conjugation is characterized by the relation

$$\eta_d^{(\text{GSR})}(\vec{r}) |G_d(\vec{r})|^2 : \eta_g |G_g|^2 \sim |G_g|^2 : |G_d(\vec{r})|^2, \quad (28)$$

so that only the rim of the diffraction aperture is imaged for the reference-to-object intensity ratio that is large enough (that determines a diffraction efficiency η_g).

Thus, the ratio of the diffraction efficiencies of a QH-PCM within the directly illuminated area and at the geometrical shadow region, being proportional to the second, the third and the fourth degrees of intensities of the geometrical optics wave and the EDW (see Eqs. (24)–(26)) are not compensated by the intensity ratio of the parts of the readout wave. Let us emphasize again that Eq. (25) explains the fact that the observed reconstruction does not result from readout of a hologram by the geometrical optics wave, but it is just the self-conjugated replica of a part of the EDW propagating into the geometrical shadow region.

The QH-based virtual dark-field effect has recently been discussed and demonstrated for the case of a thin off-axis QH recorded in a far field of a diffraction aperture [16], [30]. Namely, a QH was recorded at the plane where the primary quasi-point source was imaged. In such an arrangement, the directly illuminated area (within which the geometrical optics wave is only defined) is reduced to the central diffraction maximum of a Fraunhofer pattern, while the rest of this pattern is uniquely determined as the result of an intermodulation among the wavelets associated with different edge retransmitters of the obstacle. In the case of a far-field QH, both components of the EDW, that are out-of-phase by π , are involved into holographic imaging providing the combination gratings of equal diffraction

efficiencies. As a result a two-lobe PC-image is reconstructed, being in quite an agreement with the predictions made when accounting for the known phase structure of the EDW [8]. Therefore, it has been shown that the use of the quadratic component of the hologram's amplitude response for the case corresponding to Eq. (28) (when the part of a hologram with lower diffraction efficiency is read out by the wave with higher intensity and vice versa) provides much better edge enhancement in the resulting image than the use of the linear cross-gratings even if these gratings are illuminated by the beam of uniform intensity. Amplification of the virtual dark field effect is naturally explained if Eq. (24) is taken into account.

Note that the double-contouring effect has also been observed in some recent implementations of the newest optical wavelet-transform technique [36]. However, this effect does not find any physical explanation in the cited work. In our opinion, it is unambiguously connected with the Young–Rubinowicz interpretation of diffraction phenomena, one of the consequences of which is developed in the present study.

Let us point out here an important distinguishing feature of the near-field QH-PCM reconstruction following from Eq. (25). In accordance with the above consideration, the part of the EDW propagating in the directly illuminated area records its partial hologram with a standing reference wave at the powerful background produced by the geometrical optics wave. In contrast, a partial PCM for the EDW recorded in the geometrical shadow region is not affected by the primary wave and, as a consequence, possesses much higher diffraction efficiency (see Eq. (25)). Thus, it is just the component of the EDW propagating into geometrical shadow region that gives the main contribution to the self-conjugate response of a QH. In other words, a *unilateral* integral transform [37], [38] of the self-conjugated replica of the object wave corresponding to its propagation from the QH domain to the image plane is realized. For this reason, one can expect the singly-contoured self-conjugate reconstruction of a near-field QH recorded with a standing reference wave and read out by the object wave.

3.2.2. Distributivity of a holographic recordings

Let us explicate once more the consequences of the Young–Rubinowicz concept of diffraction phenomena relevant to the case of a near-field QH-based self-conjugation, taking account of the SPP. In contrast to the self-conjugation of a field produced by a diffuse object [3], in the case of a QH-based PC of a near-field diffraction wave, the combination gratings with the wave vectors $\vec{F}_{GQ}^{(+)}$ (see Fig. 1c) are formed only in separate areas of the recording media, as may be shown by applying the “reflection rule” [9], [25] to the diffraction device of certain configuration. In other words, the combination gratings resulting from a nonlinear mixing of the transmitting and reflectance cross-gratings of *different* edge retransmitters are weakly represented at the spatial-frequency structure of a hologram being of negligible diffraction efficiency. As a consequence, a holographic recording distributivity intrinsic to holograms of speckle-fields [18] turns out to be considerably reduced. In fact, the information on an amplitude and phase of each edge retransmitter is coded in the parameters of an interference pattern (\equiv holographic cross-grating) only along the

axis that is perpendicular to the tangent of the diffraction obstacle's rim at the corresponding critical point of the second kind and to the ray drawn from the primary quasi-point source to this critical point [10]. In this sense, the holographic recording distributivity reduces from two-dimensional to one-dimensional one. Thus, the probability for several wavelets associated with different edge retransmitters to have significant amplitude at any common point of the geometrical shadow region (that would provide sufficient intermodulation for associative properties of such a recording) is negligible, as it is seen from a "fanning" structure of a diffraction pattern [25]. Considering the "light fans" [25] associated with each of the edge retransmitters, one can see predominant overlapping of them within the directly illuminated area, *i.e.*, just within the region of low diffraction efficiency of a partial hologram of the EDW (for the reasons explained in Sect. 3.2.1). As a result, the wavelets with the wave vectors \vec{k}_g , \vec{k}_p are rescattered predominantly into their own phase-conjugated replicas, whose wave vectors are $-\vec{k}_g$, $-\vec{k}_p$, respectively (see the first and the third fragments in Fig. 1d). Thus, a near-field QH-based PCM possesses the reduced associative properties. The last conclusion found unambiguous (although indirect, in the context of a quadric holography) confirmation in a linear referenceless Young fractalography technique [15].

4. Experiment

The possibility for the EDW to be self-conjugated by using a near-field QH-PCM has been verified by us experimentally in the arrangement shown in Fig. 2. A coherent radiation from a He-Ne laser L ($\lambda = 0.6328 \mu\text{m}$, power $\sim 30 \text{ mW}$) is

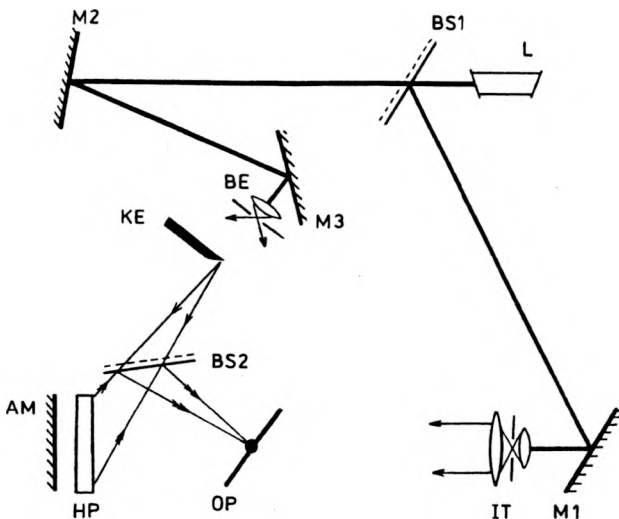


Fig. 2. Experimental arrangement for recording a QH-PCM and implementing self-conjugation of the EDW: L – laser, M1, M2, M3 – mirrors, BS1, BS2 – beam splitters, BE – beam expander, IT – inverse telescopic system, AM – autocollimating mirror, KE – diffraction obstacle (profiled knife-edge), HP – holographic plate, OP – observation plane.

split by the beam-splitter BS1 into two beams of considerably different intensities. The beam of higher intensity, being expanded using a beam expander BE consisting of a microobjective ($20\times$) and a pinhole as a spatial filter (diameter $\approx 14\ \mu\text{m}$), illuminates a diffraction device, an opaque metallic profiled knife-edge in our first experiment (see Fig. 3a). The resulting diffraction field behind the screen $G(\vec{r})$ lends itself to recording a near-field Young hologram, as shown in [10]. But now we use two complementary reference beams to form a QH-PCM. Namely, another beam of lower intensity passing through an autocollimation system (an inverse telescopic system, IT, and an autocollimating mirror, AM, just behind the holographic photoplate) produces two counterpropagating plane reference waves. The registration domain is chosen in such a manner that all three exposing waves are mutually coherent. The mean reference angles in our experiments were $0.25\ \text{rad}$ for a partial transmittance hologram $\{G^*(\vec{r})\Omega_A(\vec{r})+c.c\}$, and $(\pi-0.25)\ \text{rad}$ for a partial reflection hologram $\{G^*(\vec{r})\Omega_B(\vec{r})+c.c\}$. The reference-to-object intensity ratio is properly chosen to provide a nonlinear holographic recording; namely, $|\Omega_A|^2 \approx |\Omega_B|^2 : |G_d|^2 \simeq 1:10^2$ within the directly illuminated area, and $|\Omega_A|^2 \approx |\Omega_B|^2 : |G_d(\vec{r})|^2 \simeq 1:1$ for the diffraction angle $\vartheta_{\text{diff}} \approx 0.06\ \text{rad}$ in the geometrical shadow region.

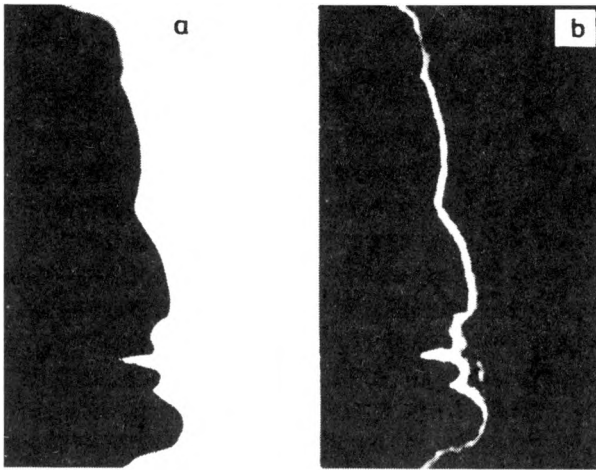


Fig. 3. Diffraction obstacle (a) and the self-conjugation reconstruction produced by the QH-PCM (b).

Holograms were recorded using the holographic photoplates Micratt LOI-2 exhibiting complex (amplitude and phase) modulation of the readout wave, with the predominant phase component of a photoresponse. Exposure time was $\sim 1\ \text{min}$, and development duration using a holographic developer GP-2 was $\sim 10\ \text{min}$. Under such conditions, a nonlinear holographic recording is provided, and the set of combination gratings, including ones with the wave vectors $\vec{F}_G^{(+)}$ and $\vec{F}_Q^{(+)}$ (see Fig. 1b), arises in the spatial-frequency structure of a hologram. We checked the presence of the valued nonlinear component of the hologram's amplitude response before performance of the self-conjugation of the object wave front through

illumination of the developed and fixed hologram with the plane wave and observation of the higher diffraction orders (up to the third, in our experiment) in transmittance.

Then, a nonlinearity recorded hologram returned to its initial position (HP, in Fig. 2) and read out by the object wave, in the absence of the reference beams. The beam-splitter BS2 (introduced already at the recording stage to avoid undesirable phase distortions of the recorded \equiv read out object wave) now serves to decouple the PC reconstruction at the observation plane OP. As is seen from Fig. 3b, this reconstruction is contoured. A careful study of the imaging process for this case (by blocking different parts of a hologram) shows that the area of a hologram corresponding to the geometrical shadow region of the recorded near-field pattern possesses predominant diffraction efficiency η_d , in accordance with the predictions in Sect. 3.2.1. It has been found that the maximal diffraction efficiency of a QH-PCM for a partial hologram of the EDW in the geometrical shadow region reaches 3% in the vicinity of the diffraction angle $\vartheta_{\text{diff}} \approx 0.06$ rad corresponding to the reference-to-object intensity ratio at the recording stage close to unity. At the same time, a diffraction efficiency measured in the directly illuminated area did not exceed 0.01%. It explains the fact that the singly contoured image is observed at the PC reconstruction rather than the doubly contoured one, as it would be expected proceeding from the Rubinowicz's representation of a diffraction integral (see Sect. 3, and refs. [8], [9], [12], [16]). The precisely measured transfer function of a near-field QH-PCM will be reported elsewhere; here we only note the result of qualitative observations consisting in gradual decreasing of a diffraction efficiency of the QH both for larger diffraction angles and for smaller ones in respect of the ϑ_{diff} which corresponds to the maximal QH-PCM's reflectivity. Let us note that the rather moderate diffraction efficiency of the QH-PCM of the EDW corresponds to the dark-field reconstruction, so that the contour image observed at dark background always possesses a contrast close to unity. Besides, owing to the above mentioned conditions of a nonlinear holographic recording, a QH is read out by relatively powerful object wave that results in acceptable energetic parameters of the QH-based self-conjugation process. At last, a diffraction efficiency of a QH-PCM can be undoubtedly increased if any thicker recording media are used, *i.e.*, if the length of interaction of the readout wave with a hologram structure [2], [5], [18] is increased.

Bearing in mind the promising applications of the Young hologram technique to preprocessing of fractal-containing optical signals [13], [15], [16], on the one hand, and for the sake of comparison of the obtained results with the early demonstrated near-field Young hologram reconstructions from a closed aperture [10], on the other hand, we performed one more experiment using the fractally bounded aperture (for definition and properties see [39], [40]) as the input signal. An aperture shown in Fig. 4a is bounded by the triadic Koch curve of the second level. Note that the structural self-similarity intrinsic to fractals is now associated just with the aperture's rim having a non-integer dimension, while the aperture itself has an Euclidean dimension "two". In this experiment, the fractally bounded aperture replaces the profiled knife-edge used in the previous experiment. Thus,

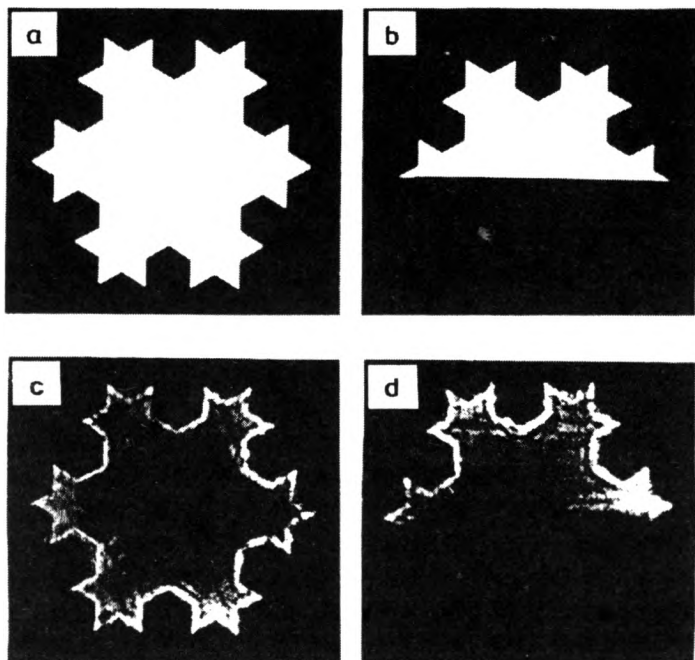


Fig. 4. Fractally bounded aperture (a), its partial version (b), and the self-conjugated reconstructions produced by the QH-PCM read out by the whole stored signal (c) and its part (d).

the wave parameter defined [41] as the ratio of radius of the central Fresnel zone constructed at the aperture plane from the center of a hologram plane to the mean linear size of an aperture (estimated as the mean value among the radii of the inscribed and overscribed circles with respect to the fractal's initiator [15]) was $\approx 5 \times 10^{-2} \ll 1$, *i.e.*, a near-field approximation was valid. All other parameters of the experiment were the same as in the previous case. Figure 4c demonstrates the PC-response of a QH reconstructed by the whole input signal. One can see again the pronounced contouring effect in this reconstruction. Besides, it has been observed that when part of the diffraction aperture is blocked, the corresponding fragment of the PC image disappears also. This is shown in Fig. 4d demonstrating the result of a PC-reflection of a half of the stored memory shown in Fig. 4b from a QH. This result confirms the conclusion that the near-field QH-PCM does not possess the associative properties due to reduced distributivity of a holographic recording in the case of interest, as it has been predicted on the basis of the SPP (see Sect. 3.2.2).

5. Conclusions and discussion

It has been shown that a nonlinear holographic recording of a near-field diffraction wave with a standing reference wave provides a self-conjugation of the object wave. In such a manner, the ability of a static nonlinearly recorded hologram to produce a PC-replica of the wave that does not obey Gaussian statistics has been

verified. In contrast to a self-pumping SBS-PCM, the PCM-properties of a QH are provided by the use of two counterpropagating reference waves. Namely, the object wave produces cross-gratings with each component of a standing reference wave, and a nonlinear mixing (spatial-frequency heterodyning) of these cross-gratings due to the quadratic component of a QH's complex amplitude response results in the combination ($2k -$) gratings constituting a PCM and satisfying the Bragg condition.

Further, it has been shown that a proper choice of the reference-to-object intensity ratio for a QH recording, on the one hand, and exploiting the quadratic component of a QH's complex amplitude response, on the other hand, provide predominant self-conjugation of the EDW and result in the contoured PC-reconstruction of a QH. Thus, the virtual dark-field effect is realized owing to a strong dependence of diffraction efficiency of the combination gratings on the modulation percentage of these gratings (the actual dependence turns out to be equal to the squared one inherent to linearly recorded holograms).

In comparison with the initial version of the Young hologram technique introduced in [10], [11] and based on a linearly recorded near-field diffraction pattern, the technique substantiated here possesses several important advantages. At first, implementation of the "soft" blocking of a powerful primary wave by balancing diffraction efficiencies of partial holographic gratings rather than the use of any "hard" blocking screen provides better (more uniform in intensity) contour reconstruction that may be seen from comparison of Figs. 3 and 4 with the referenceless Young hologram reconstructions shown in Figs. 4 and 5 in [10], respectively. Actually, as it may be shown using a SPP, the parts of the rim of the profiled knife-edge which are perpendicular to the edge of a hard blocking screen are not reconstructed or, at least, are characterized by much lower intensity than the parts of the rim parallel to the edge of a blocking screen. On the contrary, the area of a QH recorded with a standing reference wave where diffraction efficiency of the combination gratings constituting a partial PCM for the EDW reaches maximal values is "self-tuned" towards the profile of the diffraction obstacle, being involved as a whole in the reconstruction process. Besides, the implementation of apodized pupil function corresponding to the known angular dependence of the EDW's amplitude function relieves the self-conjugated image of undesirable secondary diffraction maxima often observed in referenceless Young hologram reconstructions. Further, the QH-based contour imaging is more flexible than the referenceless Young hologram-based one being implemented without any restrictions at the distances from the primary quasi-point source to the registration plane and from the diffraction device to this plane. (Let us remind that in [10] special recording geometry was implemented to provide the real conjugate image, for which a dark-field observation would be realized by the use of a blocking screen at the Young hologram plate). Finally, in the case of a QH-PCM the EDW is reconstructed mainly by the part of a hologram corresponding to the geometrical shadow region, while in the case of a referenceless Young hologram the EDW is reconstructed by the part of a hologram corresponding to the directly illuminated area. In both cases,

a singly contoured image is reconstructed, as only one of two components being out-of-phase by π of the EDW is involved into imaging process. However, diffraction efficiency of a referenceless Young hologram elsewhere far from the geometrical shadow boundary occurs to be rather low due to large intensity ratio of the geometrical optics wave and the EDW. On the contrary, a diffraction efficiency of the QH-PCM for the EDW may reach considerable magnitude at any areas within the geometrical shadow region (where Eq. (9) is valid) being limited, in principle, only by saturation of a photoresponse of the recording material used.

In comparison with far-field referenceless Young hologram [12], [15], one can note (apart from the above mentioned singly contoured image as the result of unilateral integral transform of the object wave) reduced distributivity of holographic recording explained as a consequence of validity of the SPP, and following from it reduced associative properties.

One more comparison may be performed, just with a quadric thin off-axis Young hologram [16], [30]. As it has been pointed out in [16], the edge-enhancing conjugate self-imaging based on such a hologram exhibits admissible aberrations (first of all, astigmatism of inclined rays and field curvature) only in the case when the double mean reference angle is small enough. This conclusion follows from the well-known statements of geometrical optics of holograms [42]–[44], according to which only the main image is aberration-free even if a hologram is read out in the wave length and geometrical conditions of the recording, and aberrations intrinsic to the conjugate reconstruction are minimized only in the case of paraxial imaging. It is clear that the self-conjugated response of a QH-PCM is aberration-free as the reconstructed beam differs in direction from the readout one by 180° , so that paraxial approximation is provided automatically.

In conclusion, let us point out some promising areas of application of the QH-PCM technique. Firstly, a QH-based PCM may be used in a PC-microinterferometry [45] to accurate measurements of the object's macro- and microforms. Most of the advantages of using a QH-PCM in comparison with a common holographic interferometry are shared by the technique introduced in [45]. However, since a QH is read out only by the object wave rather than two counterpropagating reference waves (as in [45]), the system operates in a one-channel regime, and its sensitivity to environmental disturbances as well as to optical misalignments becomes considerably lower. Secondly, the technique introduced may form the basis of improved fractalographic methods [46], both for revealing the self-similar components of the object of interest, and for pre-processing of fractal-containing signals.

References

- [1] REINTJES J.F., *Nonlinear Optical Parametric Processes in Liquids and Gases*, Academic Press, New York 1984.
- [2] YEH P., *Introduction to Photorefractive Nonlinear Optics*, Wiley, New York 1993.
- [3] POLYANSKII P. V., *Opt. Spectrosc.* **84** (1998), 346.
- [4] POLYANSKII P.V., *J. Opt. Technol.* **64** (1997), 28.
- [5] ZEL'DOVICH B.YA., PILIPETSKY N.F., SHKUNOV V.V., *Principles of Phase Conjugation*, Springer, New York 1985.

- [6] FISCHER B., STERNKLAR S., WEISS S., *IEEE J. Quantum Electron.* **25** (1989), 550.
- [7] RUBINOWICZ A., *Ann. Phys.* **53** (1917), 257.
- [8] RUBINOWICZ A., *Nature* **180** (1957), 160.
- [9] BORN M., WOLF E., *Principles of Optics*, Pergamon Press, Oxford 1969.
- [10] POLYANSKII P.V., POLYANSKAYA G.V., *Opt. Appl.* **25** (1995), 171.
- [11] POLYANSKII P.V., POLYANSKAYA G.V., *Proc. SPIE* **2647** (1995), 503.
- [12] POLYANSKII P.V., POLYANSKAYA G.V., *J. Opt. Technol.* **64** (1997), 52.
- [13] POLYANSKAYA G.V., *Proc. SPIE* **3317** (1997), 251.
- [14] BOGATIRYOVA G.V., *Proc. SPIE* **3573** (1998), 170.
- [15] ANGELSKY O.V., KONOVCHUK A.V., POLYANSKII P.V., *Pure Appl. Opt.* **7** (1998), 421.
- [16] ANGELSKY O.V., KONOVCHUK A.V., POLYANSKII P.V., *J. Opt. A, Pure Appl. Opt.* **1** (1999), 15.
- [17] POLYANSKII V.K., POLYANSKII P.V., *Opt. Eng.* **34** (1995), 1079.
- [18] COLLIER R.J., LIN L., BURCKHARDT C., *Optical Holography*, Academic Press, New York 1971.
- [19] WOLF E., MANDEL L., BOYD R.W., HABASHY T.M., NIETO-VESPERINAS M., *J. Opt. Soc. Am. B*, **4** (1987), 1260.
- [20] RUBANOV A.S., SEREBRYAKOVA L.M., *Opt. Spectrosc.* **79** (1995), 1009.
- [21] MIYAMOTO K., WOLF E., *J. Opt. Soc. Am.* **52** (1962), 615.
- [22] MULAK G., *Optik* **76** (1987), 143.
- [23] MULAK G., *Proc. SPIE* **1991** (1994), 7.
- [24] HONL H., MAUE A.W., WESTPFAHL K., *Theorie der Beugung*, Springer, New York 1961.
- [25] SOMMERFELD A., *Vorlesungen über theoretische Physik, Band 4, Optik*, Academic Press, New York 1954.
- [26] RUBINOWICZ A., *J. Opt. Soc. Am.* **52** (1962), 717.
- [27] KELLER J.B., *J. Opt. Soc. Am.* **52** (1962), 116.
- [28] FEINBERG E.L., *Propagation of Radiowaves along Earth Surface* (in Russian), USSR Acad. Sci., Moscow 1961.
- [29] VAGANOV R.B., KATSENELEBAUM B., *Principles of the Diffraction Theory* (in Russian), [Ed.] Nauka, Moscow 1982.
- [30] POLYANSKII P.V., *Opt. Spectrosc.* **85** (1998), 854.
- [31] KAMSHILIN A.A., PETROV M.P., STEPANOV S.I., *Proc. Eleventh USSR School on Holography*, LIAF, Leningrad 1971, 219
- [32] JUTAMULIA S., GREGORY D., *Opt. Eng.* **37** (1998), 49.
- [33] VIENOT J.C., BULABOIS J., PERRIN G., *C.R. Acad. Sci. Paris* **263B** (1966), 1300.
- [34] LOWENTHAL S., BELVAUX I., *Extrait de la Revue d'Optique* **1** (1967), 1.
- [35] VIENOT J.C., SMIGIELSKI P., ROYER H., *Holographie Optique*, Dunod, Paris 1971.
- [36] YE A., CASACENT D., *Opt. Eng.* **33** (1994), 8226.
- [37] MERTZ L., *Transformations in Optics*, Wiley, New York 1965.
- [38] SZU H., TEFLER B., LOHMANN A., *Opt. Eng.* **31** (1992), 1825.
- [39] SAKURADA YA., UOZUMI J., ASAKURA T., *Opt. Rev.* **1** (1994), 12.
- [40] UOZUMI J., SAKURADA YA., ASAKURA T., *J. Modern Opt.* **42** (1995), 2309.
- [41] GORELIK G.S., *Oscillations and Waves* (In Russian), State Ed. of Phys. and Math. Lit., Moscow 1959.
- [42] LEITH E.N., UPATNIEKS J., HAINES K.A., *J. Opt. Soc. Am.* **55** (1965), 981.
- [43] MEIER R.W., *J. Opt. Soc. Am.* **55** (1965), 987.
- [44] CHAMPAGNE E.B., *J. Opt. Soc. Am.* **57** (1967), 51.
- [45] KRUSCHKE O., WERNIKE G., TORSTEN H., DEMOLI N., GRUBER H., *Opt. Eng.* **36** (1997), 2448.
- [46] PEIPONEN K.E., SILVENNAINEN R., UOZUMI J., ASAKURA T., SAVJLAINEN M., *Optik* **93** (1993), 91.